A Soft Robotic Hip Exosuit (SR-HExo)

for Assistance and Rehabilitation of Human Locomotion

by

Lily Baye-Wallace

A Thesis Presented in Partial Fulfillment
of the Requirements for the Degree
Master of Science

Approved November 2021 by the
Graduate Supervisory Committee:

Hyunglae Lee, Chair
Spring Berman
Hamid Marvi

ARIZONA STATE UNIVERSITY

December 2021

ABSTRACT

The Soft Robotic Hip Exosuit (SR-HExo) was designed, fabricated, and tested in treadmill walking experiments with healthy participants to gauge effectivity of the suit in assisting locomotion and in expanding the basin of entrainment as a method of rehabilitation. The SR-HExo consists of modular, compliant materials to move freely with a user's range of motion and is actuated with X-oriented flat fabric pneumatic artificial muscles (X-ff-PAM) that contract when pressurized and can generate 190N of force at 200kPa in a 0.3 sec window. For use in gait assistance experiments, X-ff-PAM actuators were placed anterior and posterior to the right hip joint. Extension assistance and flexion assistance was provided in 10-45% and 50-90% of the gait cycle, respectively. Device effectivity was determined through range of motion (ROM) preservation and hip flexor and extensor muscular activity reduction. While the active suit reduced average hip ROM by 4^o from the target 30^o, all monitored muscles experienced significant reductions in electrical activity. The gluteus maximus and biceps femoris experienced electrical activity reduction of 13.1% and 6.6% respectively and the iliacus and rectus femoris experienced 10.7% and 27.7% respectively. To test suit rehabilitative potential, the actuators were programmed to apply periodic torque perturbations to induce locomotor entrainment. An X-ff-PAM was contracted at the subject's preferred gait frequency and, in randomly ordered increments of 3%, increased up to 15% beyond. Perturbations located anterior and posterior to the hip were tested separately to assess impact of location on entrainment characteristics. All 11 healthy participants achieved entrainment in all 12 experimental conditions in both suit orientations. Phase-locking consistently occurred around toe-off phase of the gait cycle (GC). Extension perturbations synchronized earlier in the gait cycle (before 60% GC where peak hip extension occurs) than flexion perturbations (just after 60% GC at the transition from full hip extension to hip flexion), across group averaged results.

The study demonstrated the suit can significantly extend the basin of entrainment and improve transient response compared to previously reported results and confirms that a single stable attractor exists during gait entrainment to unidirectional hip perturbations.

This thesis is dedicated to the network of support & the giants whose shoulders I stood upon to complete this work.

I'd like to thank my mother for her immense support during this trying time - I'm honored to have your mentorship. My friends and lab-mates kept me grounded through turbulent times and I would like to recognize their feedback to my design both as participants and as paper-reviewers. Andrea Rio, you kept me grounded, sane, and helped me push through tough times like no one else.

ACKNOWLEDGMENTS

Thank you to Dr. Carly Thalman for her mentorship in the design, development, and test of this suit and the writing of it's subsequent publications.

Thank you to Dr. Hyunglae Lee for his willingness to take on a complete stranger for a brand new project - one that I'm vert grateful to be apart of - in addition to his patience, coaching, and his excellent feedback on my presentations and publications.

Thank you to Dr.Spring Berman for her mentorship throughout my honor's thesis - without it, this task would have been incredibly daunting - and I appreciate her continued support of my new work.

Thank you to Dr. Hamid Marvi for teaching me the basics of modelling and control of robotics - it was the first class where I really knew this was the right degree for me and I'm grateful for his feedback in both my honors and master's theses.

Thank you to both new and graduated members of the NMHCR lab for all the ways they contributed to the successful production of this thesis - as mentors, study participants, and paper-reviewers.

TABLE OF CONTENTS

CHAPTER Page

CHAPTER Page

LIST OF TABLES

LIST OF FIGURES

CHAPTER Page

CHAPTER Page

Chapter 1

INTRODUCTION

1.1 Overview

There is a market need for effective, lightweight, compliant, and modular wearable robotics for gait assistance and rehabilitation. Over 795,000 Americans will experience a stroke annually, resulting in the presence of over 6.4 million stroke survivors reliant on the U.S. medical system Alonso *et al.* (2021). About two-thirds of these individuals will require assistance and rehabilitation to walk due to initial or persistent mobility deficits. Gait disorders can have a very high impact on patient quality of life and often results in a loss of independence, increase likelihood of injury-inducing falls, and result in a sedentary lifestyle Alonso *et al.* (2021). Development of a sedentary lifestyle increases the risk of secondary health conditions including respiratory and cardiovascular complications, bowel/bladder dysfunction, obesity, osteoporosis and pressure ulcers Baylor *et al.* (2014); Booth *et al.* (2012); Knight (2012); Sezer *et al.* (2015). These compounding ailments result in an estimated cost of $46 billion to the U.S. healthcare system for stroke treatment annually Alonso *et al.* (2021). To ensure patient quality of life and prevent future ailments, developing more effective and affordable methods of stroke rehabilitation is critical.

Gait impairments following a stroke can result in both a slower gait Brandstater *et al.* (1983); Knutsson and Richards (1979); Olney *et al.* (1994), and lack of gait symmetry of a transient and spatial nature between the legs Patterson *et al.* (2008). This lack of transient symmetry can appear as larger or smaller amounts of time spend in swing phase vs. stance phase Kim and Eng (2003); Mizelle *et al.* (2006); Patterson

et al. (2008), and lack of spatial symmetry often appears as larger or smaller step lengths, rather than step-length uniformity Hsu *et al.* (2003). Resolving gait asymmetries is the main purpose of this investigation. Conventional rehabilitation requires physical manipulation of a patient's ligaments by a therapist in a heavily repetitious manner that is inefficient, ineffective, and tiresome for the therapist Cao *et al.* (2014); Riener *et al.* (2005). Wearable robotics on the commercial market today for either gait assistance or rehabilitation are not always covered under patient's health insurance and can cost upwards of $10,000 Buesing *et al.* (2015). While exoskeletons for stroke rehabilitation are comparable in weight to other exoskeletons ($8.90 \pm 7.48 kg$) Rodríguez-Fernández *et al.* (2021), this is still a considerable amount of weight that can be inconvenient for the caregivers to transport and don/doff Rodríguez-Fernández *et al.* (2021).

1.2 Study 1: Right Leg Bidirectional Assistance for Relative sEMG Reduction and ROM Retention

1.2.1 Literature Review and Background

Current FDA approved exoskeletons for gait assistance are bulky, heavy, and expensive Rodríguez-Fernández *et al.* (2021). These systems are effective in supporting an upright stance and propelling and individual forward for those with spinal cord injuries (SPI) or other neurological disorders that make it difficult or impossible to walk without assistance Quintero *et al.* (2012); Tefertiller *et al.* (2018); Yang *et al.* (2015). For individuals who might be able to ambulate on their own but have a loss in range of motion at the hip or require another assistive device like a cane, such devices may be impractical in expense and size. Slight reduction in muscular effort during walking, provided by a lightweight and affordable wearable robot, may

improve quality of life and reduce falls for such individuals Power *et al.* (2016).

A variety of metrics can quantify "assistance" provided by a gait device. In Ding *et al.* (2016), reduction in metabolic output between trials with and without a soft hip exosuit quantified reduction in effort needed by the participant to move. In Thakur *et al.* (2018a), surface Electromyography (sEMG) was used to determine peak muscle electrical output in trials with and without soft hip exosuit gait assistance. In Androwis *et al.* (2018), integrated EMG (iEMG), or the area under the curve of a rectified, normalized EMG signal, was used to clinically assess an exosuit in assistance of acute stroke patients. In the protocols described below, iEMG output was found for critical hip flexors and extensors, normalized to the maximum voluntary contraction [%MVC] of the muscle of interest. In addition, it was critical to ensure that the assistive device did not hinder healthy gait biomechanics. For this investigation, hip range of motion was captured with motion capture.

1.2.2 Objective

This study had two objectives: 1) investigate potential change in muscular effort produced by hip flexors and extensors in motion with and without the exosuit; 2) assess any change in hip range of motion caused by use of this suit

1.2.3 Hypotheses

It was hypothesized that 1) the suit would provide statistically significant reduction in electrical activity read by key muscles ($\geq 5\%$) while 2) maintaining a subject's natural range of motion.

1.3 Study 2: Right Leg Unidirectional Perturbation for Basin of Entrainment Expansion

1.3.1 Literature Review

Current robot-aided gait therapies primarily utilize position controllers implementing predefined kinematic trajectories or impedance/admittance controllers that manipulate the degree of resistance or assistance during gait training Thalman and Artemiadis (2020). To allow the natural oscillatory dynamics of walking, a novel approach using the entrainment phenomenon was introduced in Ahn and Hogan (2010) to facilitate active patient engagement and prevent assistance rejection Ahn and Hogan (2012); Lee *et al.* (2019); Ochoa *et al.* (2017); Thalman *et al.* (2021b).

Entrainment is the synchronization of a pair of periodic systems, which occurs when the period of oscillatory stimuli is close to another system's natural oscillatory dynamics. This behavior has been observed in both mechanical Bennett *et al.* (2002) and biological (specifically, human) systems Ahn and Hogan (2012); Lee *et al.* (2019); Nishimura *et al.* (2018); Ochoa *et al.* (2017); Thalman *et al.* (2021b); Thorp and Adamczyk (2020). Entrainment can be used in gait rehabilitation by encouraging gradual synchronization of an impaired gait to a series of periodic perturbations that encourage faster and more symmetric gait patterns.

Previous gait entrainment studies utilizing perturbation-inducing wearable exoskeletons/exosuits have demonstrated success of this paradigm in inducing entrainment in both healthy individuals and patients who exhibit gait abnormalities following neurological impairments Ahn and Hogan (2012); Ahn *et al.* (2011); Ochoa *et al.* (2017); Thalman *et al.* (2021b).

Ahn and Hogan (2012) utilized a rigid ankle robot to entrain healthy adults in treadmill walking and a majority of subjects successfully synchronized to a series of

periodic perturbations up to 7% higher than the subject's preferred gait frequency. An overground study utilizing the same ankle robot showed that gait entrainment occurs more frequently and is induced more quickly overground than when the suit is used on a treadmill (which imposes a constant speed constraint) Ochoa *et al.* (2017). Phase-locking, or the synchronization to a particular point in the gait cycle for many consecutive steps, was always observed around toe-off phase in both treadmill and overground studies, which suggests a strong, stable point attractor Ahn and Hogan (2012); Ochoa *et al.* (2017). This rigid ankle robot was used in a successful, slightly modified test protocol with stroke and multiple sclerosis patients in Ahn *et al.* (2011) to show feasibility of this paradigm for use in rehabilitation. Both patients were successfully entrained to the periodic torque perturbations applied by the ankle robot and phase-locking occurred around the toe-off phase. While these studies confirmed the potential of the entrainment strategy for gait rehabilitation, practical application of this paradigm was still limited due to limited expansion to subject basin of entrainment (around 7% of preferred gait frequency), which may be due to device weight ($3.5kg$).

To explore the impact of device weight on entrainment effectivity, a soft, lightweight ($206kg$) wearable ankle robot was tested in a comparable entrainment study Thalman *et al.* (2021b). The SR-AFO utilizes a pair of flat fabric Pneumatic Artificial Muscule (ff-PAM) actuators to provide plantarflexion torque pertubrations at the ankle joint while walking Thalman *et al.* (2021b). The device significantly out-preformed prior gait studies, achieving a "significantly wider basin of entrainment (14.2% during walking with preferred speed and about 40% with increased treadmill speed proportional to the increase in perturbation frequency) and a faster transient response (the number of strides until the onset of phase-locking was 22 when averaged across all test conditions)" Thalman *et al.* (2021b). As in the studies utilizing the rigid ankle

robot, phase-locking was always found around toe-off phase Young and Ferris (2017).

To test the applicability of the entrainment paradigm outside of the ankle joint, a recent study investigated gait entrainment to periodic perturbations applied at the hip. The hip joint provides approximately 40% of the biomechanical power required in healthy human walking, which is comparable to the power supplied by the ankle joint for speeds between 0.8-1m/s Farris and Sawicki (2012). In this study, a lightweight yet rigid hip robot provided flexion and extension perturbations to both hip joints in cross-lateral pairs, switching orientation of the perturbations every stride in overground walking Lee *et al.* (2019). Rather than increasing the perturbation by some percent of the subject's preferred gait, a fixed torque pulse of 25ms faster than the preferred stride period was utilized. While over 70% of trials using this protocol showed successful entrainment, phase locking was observed around two distinct gait phases ($\approx$ 52% and 79%) instead of one at toe-off ($\approx$ 60%) as in prior literature. Transient response of this system was slower than results from literature and sometimes more than 50 strides were needed until the onset of phase-locking. Although this study presented compelling evidence for the potential of hip-located perturbations for entrainment induction, this paper did not present an investigation of basin expansion potential, nor did it include a clear explanation for the two distinct gait phase attractors found during entrainment. This study built the studies previously described and the development of the soft robotic hip exosuit (SR-HExo) in Thalman *et al.* (2021a) to investigate the capabilities of hip-based gait entrainment.

1.3.2 Objectives

This study had three objectives: 1) Investigate the number of stable-point attractors in gait entrainment induced by hip-based perturbations applied on a single leg in a single direction (either flexion or extension), as in previous ankle studies Ahn

and Hogan (2010, 2012); Ahn *et al.* (2011); Thalman *et al.* (2021b); 2) Investigate the extent to which the SR-HExo can induce a faster transient response and expand the basin of entrainment beyond the results with the rigid hip exoskeleton device; and 3) Investigate if entrainment and phase-locking occur statistically differently for perturbations applied in extension versus flexion.

1.3.3 Hypothesis

The first hypothesis of this study is that a single stable point attractor exists during gait entrainment to unidirectional hip perturbations. Secondly, this study hypothesizes that this lightweight, soft robotic hip exosuit can make the transient response to entrainment faster and expand the basin of entrainment further than previous reported values. Last, this study hypothesizes that phase-locking occurs at distinct times in the gait cycle for different perturbation directions.

1.4 Outline

The remainder of this thesis is structured as follows: Chapter 2 describes the design and development of the exosuit and characterization of its actuators. Chapter 3 describes the methodology, results, and discussion in separate sections for a study characterizing the assistive capabilities of the exosuit on the right leg for healthy human adults walking on a treadmill. Chapter 4 describes the methodology, results, and discussion in separate sections for a study investigating the characteristics of and potential for entrainment to hip based perturbations in healthy human adults walking on a treadmill. Lastly, conclusions from both studies are presented in Chapter 5.

Chapter 2

DEVICE CONSTRUCTION & CHARACTERIZATION

2.1 Design Construction

The SR-HExo is constructed from fabric to be a lightweight (1.80 kg), low profile (0.5 mm and 13.3 mm when the actuator is passive and active, respectively), wearable device for gait assistance and rehabilitation. The knee anchor point is constructed from neoprene, Spandex, and hook-and-loop fabric that is secured about the thigh just above the knee and translates force from the actuators to generate a torque moment about the hip (Fig. 1). The hip anchor is a pair of hook-and-loop bands that wrap securely around the user's hip and act as mounting points for both the anterior and posterior set of actuators The SR-HExo suit is actuated by flat fabric pneumatic artificial muscles (ff-PAM), as introduced and modelled by Thalman *et al.* (2021a), to assist healthy human walking during hip flexion and extension. Two pairs of ff-PAMs are used on the suit, with each pair oriented in an 'X' (known as X-ff-PAM). These pneumatic actuators contract and generate a tensile force along the length of the thigh. The resultant torque of these actuators can be estimated as $\tau = Fr_{thigh}$, where τ is the torque applied to the hip by the SR-HExo, F is the tensile force generated by actuator contraction, and r_{thigh} is the perpendicular lever arm distance from the center of the hip joint to the leading edge of the thigh at the knee anchor point, which is half the thickness of the user's thigh Thalman *et al.* (2021a).

These X-ff-PAM are positioned anterior and posterior to the right hip as shown in Fig. 1, providing an assistive torque in flexion and extension respectively. In flexion, the exosuit mimics the shape and behavior of the Iliacus (IL), Rectus Femoris (RF),

Table 2.1: Functional Requirements, Considerations, and Constraints for the Design of the SR-HExo

Design Requirements	Characteristics
Design Considerations and Criteria	
Soft, compliant	Neoprene, Spandex and Nylon material
Low profile	$\sim 5\ mm$
Easy don/doff	$\leq 60\ s$
Light weight	$\leq 1.8\ kg$
Motion and Force/Torque Considerations	
Hip Flexion (Flx.)	0.66 Nm/kg @ 5.5% of gait cycle
Flx. Muscle Assistance	Iliacus (IL), Vastus Medialis (VM), and Rectus Femoris (RF)
Hip Extension (Ext.)	0.56 Nm/kg @ 51.6% of gait cycle
Ext. Muscle Assistance	Gluteus Maximus (GM) and Biceps Femoris (BF)
Minimum ROM	40^o (30^o Flexion, 10^o Extension)
Controls Criteria	
Perturbation Timing	0.2 - 0.3 *sec* actuation time
Flx. Actuator Timing	50-90% of gait cycle
Ext. Actuator Timing	10-45% of gait cycle
Flx. Force (F_{flx})	$\pm$ 10% of 200 N
Ext. Force (F_{ext})	$\pm$ 10% of 100 N
Natural Walking Pace	$\geq$ 1.0 - 1.4 m/s

Figure 1: The SR-HExo Shown on a User from (a) the Side Profile, (b) Back View, (c) Front View, and (d) Back View. The Actuator Anchor Points and Adjustable Leg Brace in (a) Are Highly Modular to Fit Many Users. The X-ff-PAM Used for Actuation in Flexion (e) and in Extension (f) Including the Modular Knee Anchor Point

and Vastus Medialis (VM), critical hip flexors Bonnefoy-Mazure and Armand (2015); Webster and Darter (2019); Winter (1980). In extension, the exosuit mimics the shape and behavior of the Gluteus Maximus (GM), Semimembranosus (SM), and Biceps Femoris (BF), critical hip extensors Bonnefoy-Mazure and Armand (2015); Webster and Darter (2019).

For use in rehabilitation, either the posterior or anterior set of actuators can be used at a time to deliver a periodic pulse of torque. The soft robotic hip exosuit (SR-HExo) design is shown in Fig. 1. The SR-HExo actuates the posterior X-ff-PAM from 10-45% of the gait cycle to assist peak hip extension torque and the anterior X-ff-PAM from 50-90% of the gait cycle to assist peak hip flexion torque. The actuators cannot be slacked and must be mounted in tension to maximize force transmission. This

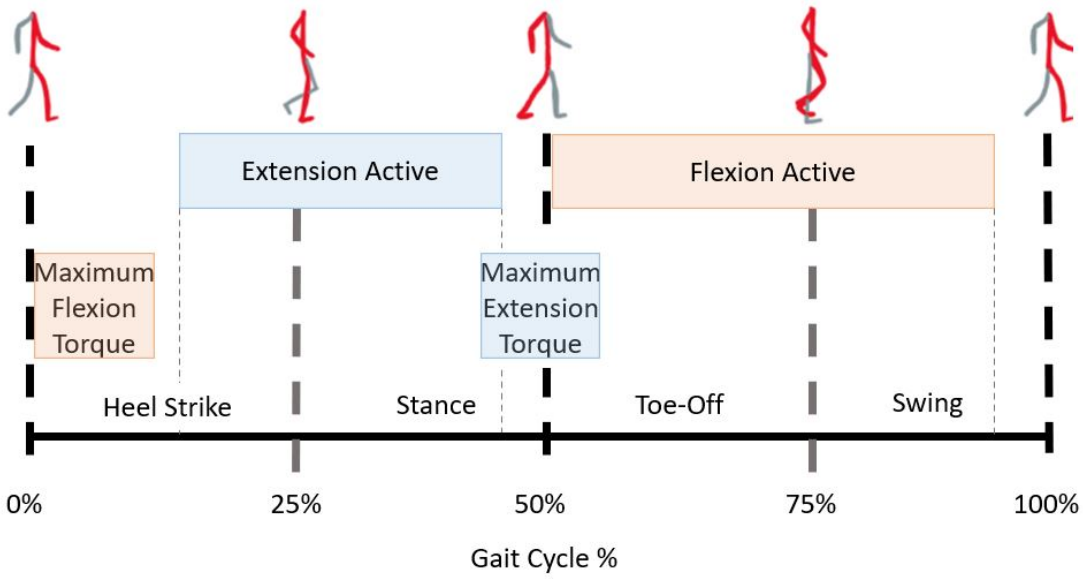

Figure 2: System State over a Single Gait Cycle from Heel Strike to Heel Strike Is Primed to Assist the Moment of Greatest Torque in Flexion and Extension Separately, Resulting in System Operation for 70% of the Total Gait Cycle

orientation also hugs the user's thigh more closely than suits that run distally down the leg as in Thakur *et al.* (2018a). The primary purpose of the X-ff-PAM orientation is to guarantee complete ROM in flexion and while preventing any disturbance to natural hip abduction/adduction Thalman *et al.* (2021a). The medial and distance placements of the actuators as well as actuator length are also adjustable given the hook and loop features shown in 1.

2.2 Actuator Characterization

The X-ff-PAM actuator orientation was tested thoroughly as in Thalman *et al.* (2019), where pairs of ff-PAM actuators had been methodically tested and used in parallel. These two designs were evaluated to compare performance for both maximum force output and dynamic response. A universal testing machine (UTM) (Instron 5565, Instron Corp., High Wycombe, United Kingdom) was used to demonstrate the proposed design could provide sufficient force output within a time window that

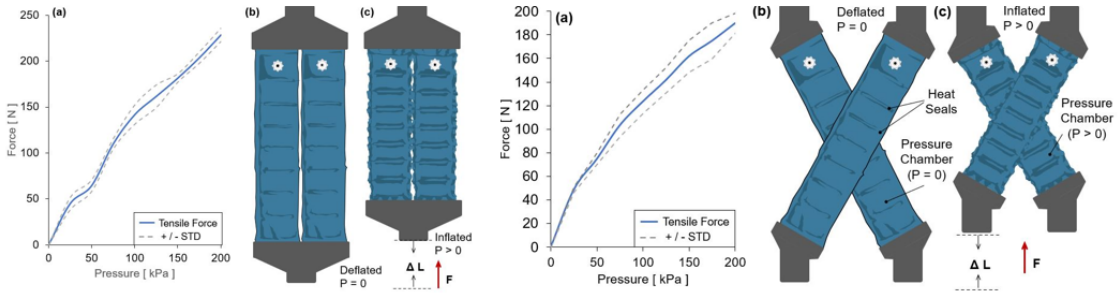

Figure 3: (1) (a) the Tensile Force of the Parallel ff-PAM at Varying Pressures Measured in the UTM, from Pressures 0 - 200 kPa in 25 kPa Increments, and the Actuators Shown in the Deflated (b) and Inflated (c) States (2) the Tensile Force of the X-ff-PAM at Varying Pressures, from 0 - 200 kPa (a), and the X-ff-PAM in the Deflated (b) and Inflated (c) States.

allowed the user to feel each controlled perturbation.

The X-ff-PAM and dual parallel ff-PAM orientations were evaluated at a quasi-static fixed length at maximum extension to produce a function of force vs. pressure to measure actuator isometric contraction. The actuators were fixed between a pair of UTM vice clamps, one stationary, and the other positioned below the load cell as in Fig. 4. Fabric-wood connectors interfaced between the actuators and vice clamps in both orientations to more accurately represent the force of the actuators as mounted on the exosuit. The parallel actuators were attached to reinforced triangles that brought the fixture to a single point at either end to be pinched in the clamp. The X-ff-PAM connected to a pair of wooden beams clamped between the vice grips at both ends to properly orient the crossing point of the actuators, as well as keep the actuators flat and taught. Actuator displacement was fixed at 0 mm and pressure was increased incrementally from 0 to 200 kPa in steps of 25 kPa to preform a quasi-static force vs. pressure evaluation Thalman *et al.* (2021a). Over three repeated trials tensile force was recorded for both actuator orientations. The average force output of the X-ff-PAM at 200 kPa was 190.2 $\pm$ 8.4 N, which is within $\pm$ 10% of the maximum force required for hip flexion force assistance (200 N) as shown in Table 1.

A dynamic test was preformed to measure actuator time response to an impulse of pressure and produce a force-time relation as shown in Fig. 4. As in the quasi-static evaluation, fabric interface connected to the top and bottom of both actuator orientations to the UTM to simulate the force loading path. The dynamic response was induced by quickly opening a 3-way, 2-channeled solenoid valve (320-12 VDC, Humphrey, USA) to rapidly deliver pre-set pressure to the inflate the air chambers of the ff-PAM. This characterization is crucial to ensure the ff-PAM delivers a tensile force through uniaxial contraction to support hip flexion and extension in the correct phases of human gait. Instantaneous pressure from the pressure source were supplied to the valves, and released in a pulse with a period of 1 *sec*, with the valve remaining open for 0.3 *sec* and closed for 0.7 *sec*. The maximum force output and latency in response of each actuator were recorded and are shown in Fig. 4 for both actuator configurations.

The parallel and X actuator orientations produced similar force responses under the same test conditions. As in Fig. 4b, the parallel actuator reached a peak force of 189.2 $\pm$ 8.2 N at an instantaneous pressure of 200 kPa over a 0.3 *sec* window, with an unloading response time of 0.46 *sec* Thalman *et al.* (2019). The X-ff-PAM orientation (Fig. 4 2.c) reached a peak tensile force of 191.2 $\pm$ 4.6 N at 200 kPa and an unloading time of 0.25 *sec*. The X-ff-PAM orientation's maximum force was within the range of force requirement for adequate hip flexion assistance in a short enough time window that will not impede upon natural human biomechanics during a typical pace of human walking.

The X-ff-PAM orientation was able to achieve the desired force requirement of (200 $\pm$ 10% N) for hip flexion assistance in a short time window that can be scaled within a typical cadence of healthy human walking.

Given these comparable operational results, the X-ff-PAM was then evaluated

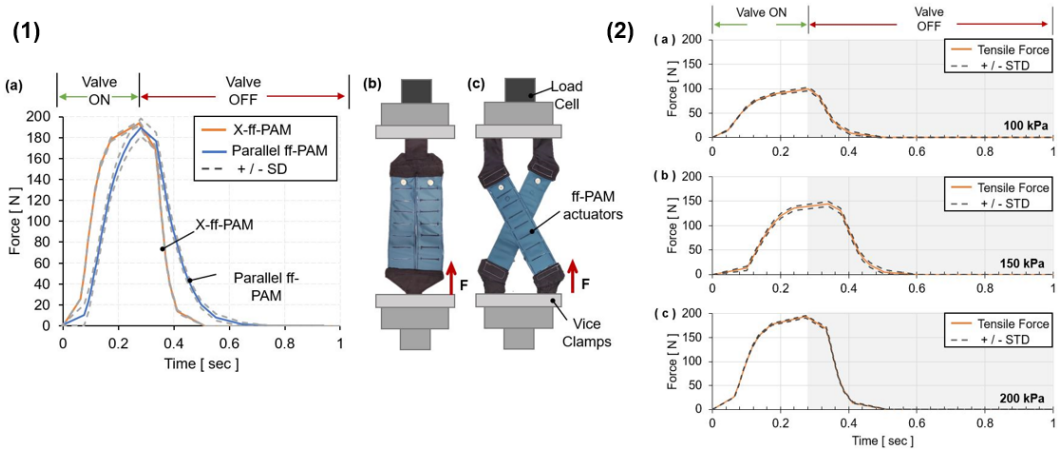

Figure 4: (1)(a) the Tensile Force Output Parallel ff-PAM (b) Compared to the X-ff-PAM (c) Recorded as a Dynamic Response to Instantaneous Pressure at 200 kPa. (2) the Tensile Force of the X-ff-PAM Recorded as a Dynamic Response to Instantaneous Pressure at (a) 100, (b) 150, and (c) 200 kPa

with further dynamic testing at varying pressure levels - 100, 150, and 200 kPa. At 100 kPa, the maximum force output was 99.4 $\pm$ 3.7 N, with a deflation time of 0.22 *sec* Thalman *et al.* (2019). At 150 kPa the peak force output was 144.1 $\pm$ 5.0 N, with a deflation time of 0.27 *sec*. Peak force at 200 kPa was measured at 193.7 $\pm$ 2.1 N, with a deflation time of 0.24 *sec*. 200 kPa was selected for use in human trials of the X-ff-PAM actuators to ensure the 200 $\pm$ 10% N force criteria was met during walking.

Chapter 3

RIGHT LEG BIDIRECTIONAL ASSISTANCE FOR RELATIVE SEMG REDUCTION AND ROM RETENTION

3.1 Summary

This study investigated the capabilities of the SR-HExo to assist in healthy human locomotion. This was quantified through muscular expenditure as measured though normalized surface Electromyography (iEMG) and range of motion as monitored with motion capture. The results indicate that the suit did significantly impact muscular effort when in the active condition, reducing iEMG for key hip flexors and extensors by greater than 5%. Some antagonist electrical behavior was found, likely due to some physical rejection to the suit. Range of motion was primarily preserved, with a 4^o shift towards flexion, likely due to suit over-tensioning. From the positive outcomes of this study, further work should increase system portability and improve range of motion.

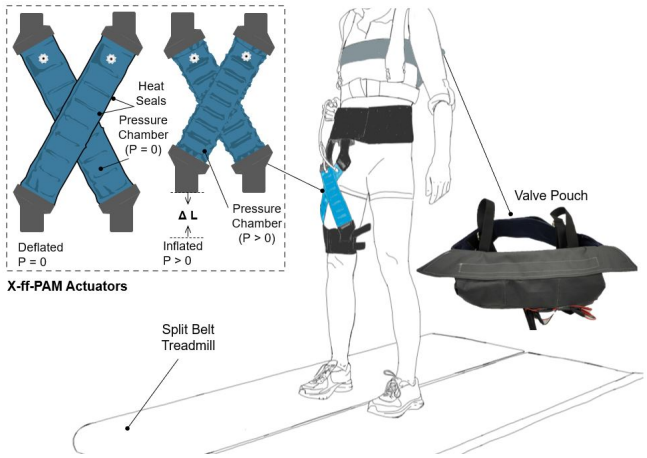

Figure 1: X-ff-PAM Actuators Shown Deflated and Actuated. The User Test Setup Is Shown on a Split Belt Treadmill, Wearing the SR-HExo on the Right Leg Just above the Knee and Wearing the Valve Pouch on the Upper Back.

3.2 Methods

This section covers the experimental methods used in this study, including the recruitment of subjects, instrumentation, control, and experimental protocol.

3.2.1 Subjects

This study was conducted with three healthy participants, the demographics of which can be found below, recruited according to the procedures for healthy participants as approved by the Institutional Review Board of Arizona State University (STUDY00012099). These individuals were (1) no younger than 18 years of age, (2) did not have any pre-existing neurological disorders or biomechanical injuries diagnosed or occurred in the last 12 months, and (3) featured no abnormal gait characteristics such as toe-walking. Two experimental protocols were implemented, each on a different day, and each subject participated in both experiments.

Table 3.1: Demographics Presented as a Range of the Three Participants in This Study

Information	Range
Age *(years)*	$21 - 27$
Weight *(kg)*	$47.6 - 83.9$
Height *(m)*	$1.68 - 1.88$
Leg length *(m)*	$0.79 - 1.05$

3.2.2 Instrumentation

The soft robotic hip exosuit with X-ff-PAM actuators both posterior and anterior to the right hip was used in this study. The suit was adjusted for each subject such

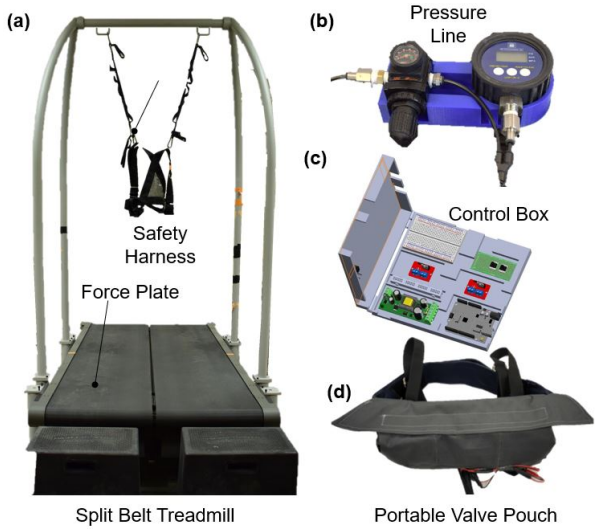

Figure 2: (a) the Split Belt Treadmill Test Setup and Safety Harness Used by Participants. (b) the Pressure Regulator and Gauge for Consistent Pneumatic Instantaneous Pressure. (c) the Control Box Which Houses All the Eletro-pneumatic Hardware, Pressure Gauge, and Pressure Regulation Hardware. (d) Wearable Pouch for Storage of Pneumatic Valves on the User

that: 1) the hook-and-loop belt wrapped around a subject's hip bone where the top of the belt was aligned with the bony protrusion at the top of the hips 2) the lower edge of the knee anchor was positioned about 5 *cm* above the bony process of the kneecap to avoid contact or pinching at the back of the knee 3) anterior actuators were attached at the midline just below the navel and at the lateral bony process of the hip 4) posterior actuators were attached at the midline near the base of the spine and at the lateral bony process of the hip as in Fig. 1b & c.

The exosuit was designed for use in rehabilitative contexts and for critical sensing and controls inputs utilized an instrumented treadmill, (Bertec Treadmill, Columbus, OH, USA), and portable air compressor (Model 8010A, California Air Tools, USA) to minimize the necessary on-board components for the user to minimize system weight. This design attempted to improve upon the actuation timing of the SR-AFO in Thalman *et al.* (2020) by mounting the pneumatic valves on the user in the low-profile fabric pouch shown in Fig. 1d. A tether, partially mounted to the treadmill

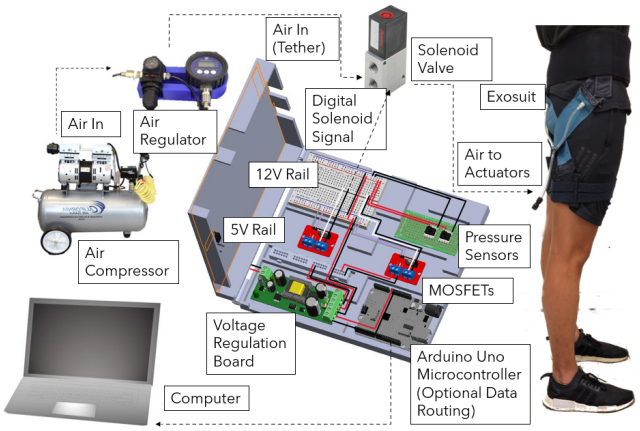

Figure 3: Overview of the SR-HExo, Electronics, and Pneumatic System Integration. Triggering of the Pneumatic Valve Is Controlled via a MOSFET Featured in the Control Box and Is Monitored by a Real-time Computer System. Back-pressure of the Portable Air Compressor Is Set Manually Before Each Trial to Ensure Appropriate Force Output.

to prevent tapping the subject, unified the pneumatic air lines, control wiring, and power source to the pouch in a single line going to the user from the air compressor and other control hardware. The other control hardware included pressure sensors (ASDXAVX 100PGAA5, Honeywell Sensing and Productivity Solutions, Charlotte, USA) in each pneumatic line to monitor actuator pressure throughout use, MOSFETs (IRF520 MOSFET Driver Module) for pneumatic valve control, with system control and monitoring of all analog inputs and digital system outputs performed by a speedgoat©(Speedgoat GmbH, Switzerland) through Simulink©(SIMULINK Research License, MATHWORKS, Natick, MA). The pressure sensors and MOSFETs were housed in the 3D printed control box (Fig. 2c) which sits beside the treadmill and is not on-board the participant.

To investigate the first hypothesis, surface electromyography measurement (EMG) (Delsys Trigno, Delsys, Natick, MA) system recorded the muscle activity of the Iliacus (IL), Rectus Femoris (RF), Biceps Femoris (BF), and Gluteus Maximus (GM), the key hip flexors and extensors respectively. To investigate the second hypothesis, a motion capture system (T40s, VICON Inc., Los Angeles, CA) monitored the right and

left hip, knee, and ankle joints with reflective markers placed anterior and posterior to the bony processes of the pelvis as well as the center of the thigh to track (in particular) hip angle in the sagittal plane.

3.2.3 Experimental Protocol

Subject experimental preparation consisted of installing and initializing surface EMG sensors, installing motion capture elements, and determining preferred gait pace. To properly scale EMG data, surface EMG sensors were placed on the belly of the muscles indicated prior and the maximum voluntary contraction (MVC) of each muscle was evaluated per standard International Electrophysiology and Kinesiology (ISEK) protocols Merletti and Di Torino (1999). Motion capture elements were placed posterior and anterior to the hip, at the centerpoint of the side of the thigh, at the centerpoint of the side of the knee, on the side of the ankle bone, at the centerpoint of the side of the calf, at the back of the ankle just above the heel, and at the ball of the foot, just inward from the big toe, with all of these markers on both legs. Subjects were asked to stand very still to initialize the connection orientation "skeleton" of each motion captured point relative to one another. Lastly, the preferred walking pace was determined by increasing the treadmill speed by steps of 0.1 m/s starting at 0.8 m/s until the subject indicated the pace was quicker than their natural cadence, then decreased by the same step size until the subject indicated it was too slow. The final baseline walking speed was selected from the average of these two values, and was between 1 and 1.3 m/s for all participants, which was within standard bounds of healthy human walking rates Farris and Sawicki (2012).

The main experiment contained three conditions: (1) no exosuit, (2) passive exosuit, and (3) active exosuit. The first two conditions were each ran once at the subject's preferred walking speed for two minutes. After a three minute resting pe-

riod to prevent muscle fatigue, the active exosuit trials were then ran. In the active exosuit condition, the extension X-ff-PAM was pressurized for 10-45% of the gait cycle, assisting only in the terminal swing to loading response and the flexion X-ff-PAM was pressurized at 200 kPa for 50-90% of the gait cycle, assisting only in the late stance phase. These actuators were depressurized for the remainder of the gait cycle to prevent any impedance upon natural gait biomechanics. The third condition was repeated three times, with three minute breaks in-between, to allow users to adjust to the device and protocol. The trial that felt most comfortable to the participant was selected for analysis and review.

3.2.4 Data Analyses

Precise perturbation timing was critical to ensure the suit provided locomotor assistance without impeding upon natural gait cycle biomechanics. This was accomplished through gait cycle calculations preformed with force plate data provided by the treadmill (Fig. 2a) in the Simulink© model. The average timing of the last previous five steps was used to determine the user's cadence and calculate the timing for the next applied perturbation. The extension actuator was activated and deactivated at 10% and 45% of the gait cycle, respectively, while the flexion actuator was activated and deactivated at 50% and 90% of the gait cycle, respectivelyThalman *et al.* (2021a).

To determine suit impact on range of motion, motion capture of the hip joint behavior was processed post-collection in MATLAB at a measurement rate of 250 Hz. Assuming that forward motion of the subject is "z", side to side motion is "x" and the height of the subject is "y", the "x" component was ignored as the subject should remain in a relatively constant position on the treadmill with respect to the centerline of the treadmill. Right leg motion capture sensors posterior and anterior

to the hip were used to generate a line in the Y-Z plane and that line's orthogonal component, which were used to compare the angle created by the line of the hips and the midpoint of thigh. This was taken as the "angle of the hip", and follows a trajectory and magnitude comparable to results found in literature Wesseling *et al.* (2015).

To determine suit impact to muscle electrical activity, surface EMG data was collected at 2 kHz, scaled, and then processed to produce iEMG data. This data was filtered using the second-order Butterworth low-pass filter with a cutoff frequency of 20 Hz and was synchronized with kinematic data and force plate data to monitor changes in muscle expenditure in the IL and RF, and BF and GM muscles across the gait cycle, with a focus on flexion and extension reduction respectively. The area under the curve was taken between the no exosuit and active conditions from 10-45% of the gait cycle for the hip extensors (GM and BF) and 50-90% of the gait cycle for hip flexors (IL and RF) Thalman *et al.* (2021a).

3.3 Results

3.3.1 iEMG Reduction

The average results for the three participants are shown in 4. EMG activity was evaluated for the BF and GM during hip extension and the reduction of %MVC was 6.6 ± 3.6% and 13.1 ± 5.1% for the BF and GM respectively. Even more impressive was the %MVC reduction achieved by the IL and RG muscles, which were 10.7 ± 1.4% and 27.7 ± 14.2% respectively.

As shown in 5, EMG results for a representative subject, there was definitive reduction in muscular electrical output (scaled to %MVC) for the Biceps Femoris and the Rectus Femoris. In the Gluteus Maximus and Iliacus there was a shift in muscular

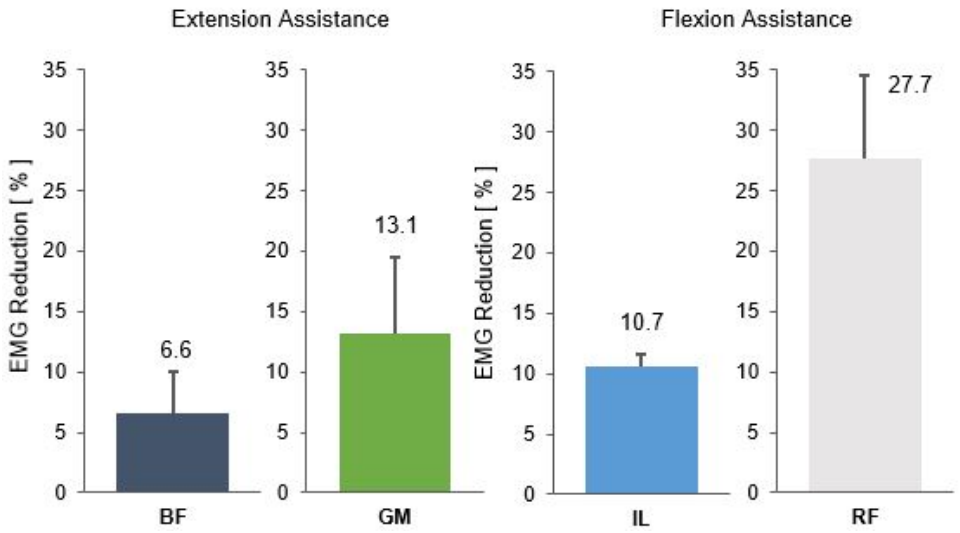

Figure 4: EMG Area Reduction from 50-90% of the Gait Cycle for Flexion Assistance of the IL and RF Muscles, and 10-45% of the Gait Cycle for Extension Assistance of the GM and BF Muscles.

activity in opposition to flexion and extension respectively. This antagonistic behavior may have been a result of lack of familiarity with the suit resulting in a slight rejection of the suit by the human body or over compensation for an unfamiliar sensation.

3.3.2 Range of Motion Analysis

All participants maintained a hip angle profile like in Fig. 6(a), which did not drastically alter from their normal ROM in the no exosuit condition and shifted only slightly in the active exosuit condition. The peak angle in hip flexion was 21.2 $\pm$ 0.5^o with no exosuit, 19.0 $\pm$ 3.9^o in the passive condition, and 19.3 $\pm$ 3.0^o in the active condition as in Fig. 6(b). The peak angle in hip extension was -11.0 $\pm$ 2.8^o without the exosuit, -6.3 $\pm$ 5.0^o in the passive condition, and -6.8 $\pm$ 3.8^o in the active condition. The target ROM for this design was the standard healthy range of motion at the hip- 30^o - but in the active exosuit condition the ROM was only 26.0^o. This slight narrowing of ROM is likely due to over-tensioning of either set of actuators, which can be mitigated with more precise actuator placement.

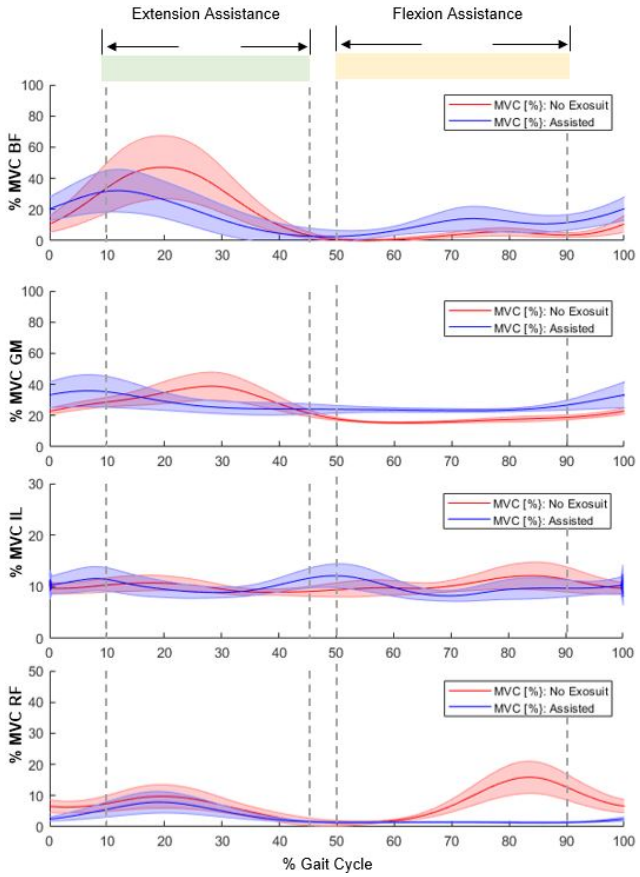

Figure 5: Relative EMG Reduction for a Representative Participant Across the Gait Cycle for the BF and GM - to Assess Extension Effort Reduction, and the IL and RF - to Assess Flexion Effort Reduction.

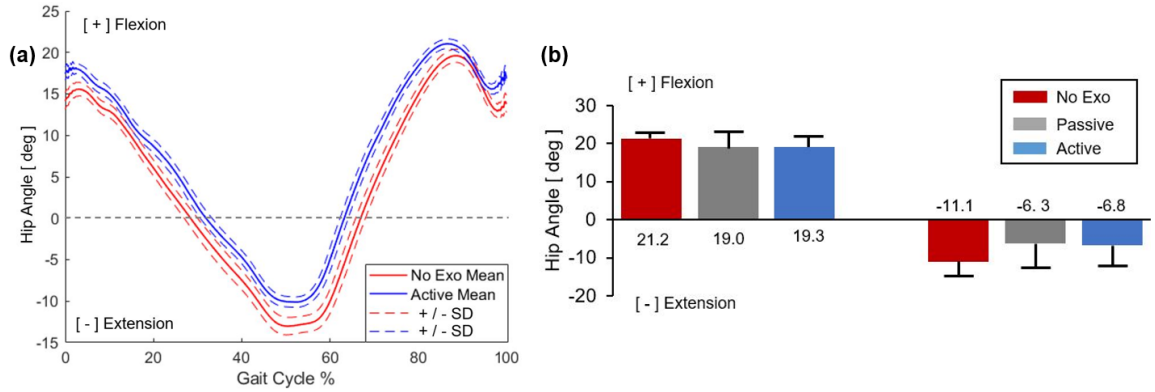

Figure 6: (a) Experimental Results of Range of Motion Monitoring at the Hip Joint with and Without the SR-HExo for a Representative Subject (b) Experimental Results of Hip Angle for All Participants for All Experimental Conditions Confirm That There Is a Minimal Impact on Rom at the Hip During Active Exosuit Usage. Error Bars Represent Mean ± Standard Deviation (SD) Across All Three Participants

3.4 Discussion

This study included the preliminary results of locomotor assistance trials with three healthy participants across three different test conditions: no exosuit, passive exosuit, and active exosuit. In the active exosuit condition, the flexion actuators were active from toe-off to terminal swing, and the extension actuators were active from stance-phase to toe-off. In this active exosuit condition, hip ROM was reduced to 26^o from the target ROM of 30^o. Normalized EMG data from key hip flexors (IL and RF) and hip extensors (GM and BF) showed significant muscular effort reduction between 50-90% and 10-45% of the gait cycle, respectively.

The minimal impact of the SR-HExo to hip ROM combined with statistically significant reductions in muscular activity during both hip flexion and hip extension indicate device potential to provide noninvasive assistance that does not impede natural gait kinematics during human locomotion. The SR-HExo has minimal moving parts, reducing the risk of pinching or shearing injuries (which are possible with cable-driven systems), in addition to being one of the lightest low-profile lower body wearable robotics with statistically significant gait assistance capabilities in the state of the art, both of which are important credentials as identified by wearable robotics users Power *et al.* (2016).

This study was limited to participants with standard locomotor behaviors and fits most, but not all users with minor adjustments. This suit does not properly fit users with legs shorter than 0.71 m and modifications to the knee anchor point, hip anchor point, and actuators must be made to maximize potential user pool.

Chapter 4

RIGHT LEG UNIDIRECTIONAL PERTURBATION FOR BASIN OF ENTRAINMENT EXPANSION

4.1 Summary

This study investigated the capability of a modified SR-HExo to expand the basin of entrainment of healthy adults via unidirectional torque perturbations applied at the hip. The SR-HExo was modified such that the valves were left with other instrumentation on a table, off of the participant, and the exosuit was donned with either the posterior or the anterior set of actuators, not both simultaneously.

Entrainment as a rehabilitative paradigm relies upon the natural synchronization of the human gait as a periodic system to periodically applied perturbations. Once the appropriate level of perturbation magnitude (determined by the level of air pressure) and perturbation frequency is determined for a given subject, this method requires no closed-loop feedback. This open-loop control scheme enables voluntary patient participation since the subject aligns gait with the robot rather than the robot predicting and reacting to the user in a closed-loop fashion. This simplistic control methodology behind entrainment is computationally cheap, requires no additional time to tune the controller parameters, and easily accessible for use inside and outside of rehabilitative facilities, potentially with more affordable controllers.

Entrainment success was quantified through phase-locking value, variability of phase-locking, consecutive strides in the entrainment window, and strides until the onset of phase-locking, and all subjects were successfully entrained in every test condition. These characteristics indicated that there was a single-point attractor to toe-off

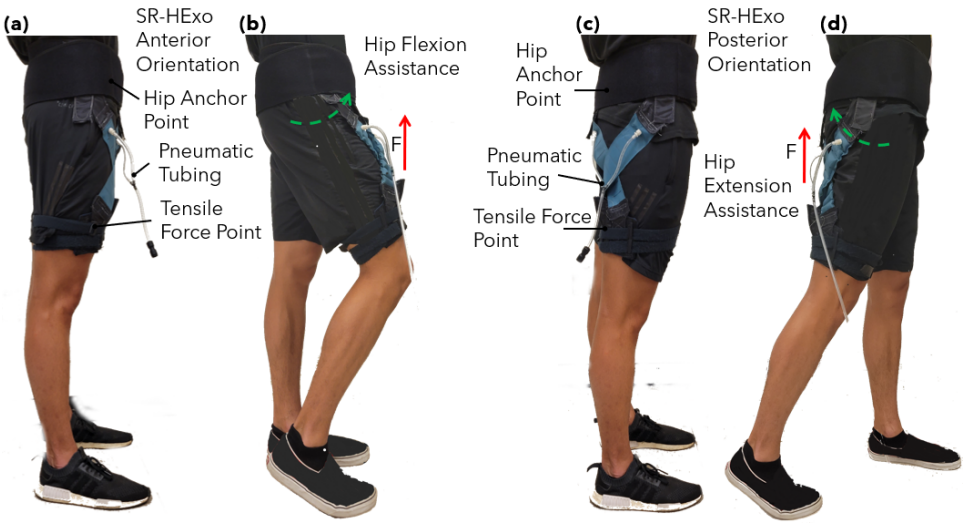

Figure 1: The SR-HExo Shown on the Right Hip of a User on (a) the Anterior Side of the Hip with Actuators Passive, (b) the Anterior Side of the Hip with Actuators Active, (c) the Posterior Side of the Hip with Actuators Passive, and (d) the Posterior Side of the Hip with Actuators Active.

phase regardless of suit orientation (anterior or posterior), but that there was a statistically significant difference in entrainment characteristics between each orientation. Perturbations applied anterior to the hip occurred more consistently, more quickly, lasted longer, and occurred around and just before 60 %GC. Perturbations applied posterior to the hip occurred slightly less consistently, less quickly, and occurred around and just after 60 %GC. From the positive outcomes of this study, further work should test the limits to which this system can expand the basin of entrainment of healthy adults, and begin preparation for clinical trials.

Note: In this study, the SR-HExo is worn over only the right hip and perturbations are only unidirectional. This is fundamentally different from the prior hip entrainment study which applied perturbations to both hips simultaneously in opposite directions every stride Lee *et al.* (2019).

4.2 Methods

This section covers the experimental methods used in this study, including the recruitment of subjects, instrumentation, control, and experimental protocol.

4.2.1 Subjects

This study was conducted with eleven healthy participants, the demographics of which can be found in the table below, according to the procedures for healthy participants as approved by the Institutional Review Board of Arizona State University (STUDY00012099). These individuals were (1) no younger than 18 years of age, (2) did not have any pre-existing neurological disorders or biomechanical injuries diagnosed or occurred in the last 12 months, and (3) featured no abnormal gait characteristics such as toe-walking.

Table 4.1: Demographics Presented as a Range of the Eleven Participants in This Study

Information	Range
Age *(years)*	$20 - 26$
Weight *(kg)*	$40.8 - 83.9$
Height *(m)*	$160.0 - 195.6$
Sex *(m/f)*	6/5

4.2.2 Instrumentation

The SR-HExo was modified to utilize only a single set of X-ff-PAM actuators on either the posterior or anterior side, and was mounted on the subject's right hip (Fig. 1). All experiments were preformed on a dual-force-plate treadmill (Bertec

Treadmill, OH, USA) that collected ground reaction force data from the right leg for stride calculations. This forceplate was calibrated prior to each experiment and was zeroed between each trial to limit noise in the data. A safety harness was used with the treadmill to prevent falls and ensure subject safety. The SR-HExo was controlled using the Simulink Real-Time System (Mathworks, MA, USA) on a real-time target machine (Baseline Real-Time Target Machine, Speedgoat, Bern, Switzerland). A portable air compressor (Model8010A, California Air Tools, USA), fitted with a 3-way, 2-channeled solenoid valve (320-12 VDC, Humphrey, USA) delivered fixed pulses of compressed air as processed by the MOSFET (IRF520 MOSFET Driver Module) driver module (Fig. 2). These controlled perturbations pressurized the chambers of the soft actuators for the specified inflation time indicated below. The tubing that passed between the air source and control module to the suit were loosely mounted on the treadmill to prevent any impedance upon natural locomotion.

The frequency of these applied perturbations are updated for each trial through the open-loop control strategy designed in Simulink (Mathworks, MA, USA). The controller provides heavily damped, gentle perturbations via the pneumatic actuators which differ from the rigid robotic torque pulses used in previous hip entrainment studies Lee *et al.* (2019).

Perturbations applied to users consisted of 0.2 *sec* pulses of inflation for the X-ff-PAM at a consistent 200 *kPa*. According to Fig. 4, this would yield about 180 N force and the corresponding hip torque is 18 Nm assuming a $10cm$ moment arm from the actuator to the hip joint. This torque value is comparable to the torque assistance provided in Thalman *et al.* (2021a), Ding *et al.* (2016) which is approximately 16% of the average maximum hip torque of healthy adults Grimmer *et al.* (2014). It is worth noting that prior hip entrainment studies were preformed with a heavier robot (2.1 kg) at a maximum hip torque of 6 Nm Lee *et al.* (2019) which is about 5% of the

average maximum hip torque of healthy adults Grimmer *et al.* (2014). As a result, the SR-HExo in this experiment has a significantly higher torque density than its rigid counterpart.

4.2.3 Experimental Protocol

The subject's preferred walking speed was determined with the same method as described in Chapter 3: Methods: Experimental Protocol. The gait cycle frequency at this preferred walking speed, henceforth referred to as the "preferred gait frequency" (f_{PWS}), was used to calculate the perturbation frequencies for testing.

This study comprised of two separate experiments, conducted in random order, with one featuring hip flexion perturbations generated by an actuator positioned anterior to the hip, and the other with hip extension perturbations generated by an actuator positioned posterior to the hip. In each experiment, six different perturbation frequencies were tested starting at a subject's preferred gait frequency ($1.0 \cdot f_{PWS}$) up to 15% higher ($1.15 \cdot f_{PWS}$) in steps of 3%. These six conditions were divided into two sets of three trials, with f_{PWS} - $1.03 \cdot f_{PWS}$ - $1.06 \cdot f_{PWS}$ and $1.09 \cdot f_{PWS}$ - $1.12 \cdot f_{PWS}$ - $1.15 \cdot f_{PWS}$ grouped together respectively. Frequencies in a group were tested in random order. The first set included perturbation frequencies close to the rate used by Lee *et al.* (2019) to evaluate if healthy subjects could successfully entrain to hip based perturbations with a rigid hip exoskeleton robot walking overground. The second set was used to evaluate the potential of the SR-HExo in extending the basin of entrainment beyond the standard healthy basin of entrainment for humans of 7%.

For each trial, subjects were instructed to walk for three minutes as comfortably as possible. They were informed that they would feel the pull of the exosuit device and allowed to adjust their step length and pace until they could comfortably walk with the device. To prevent visual entrainment, subjects were instructed to look

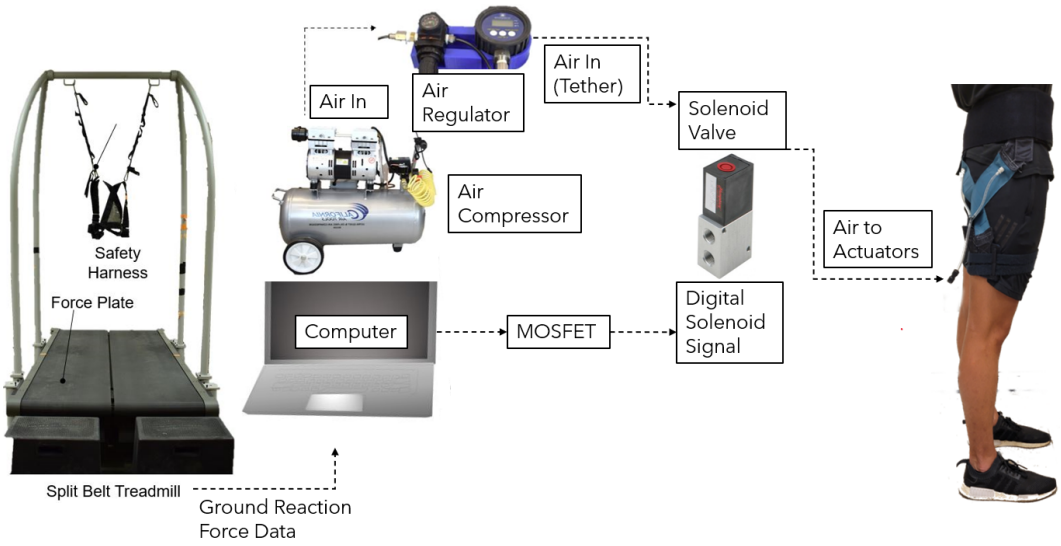

Figure 2: Overview of the SR-HExo, Electronics, and Pneumatic System Integration. Triggering of the Pneumatic Valve Is Controlled via a MOSFET Featured in the Control Box and Is Monitored by a Real-time Computer System. Back-pressure of the Portable Air Compressor Is Set Manually Before Each Trial to Ensure Appropriate Force Output.

at a blank wall and were indicated visually by the experimenters to shift left or right to maintain appropriate positioning on the treadmill. In addition, to prevent auditory entrainment, subjects wore foam earplugs (Noise Reduction Rating (NRR) of 32 decibels) and noise cancelling headphones (WH1000XM3, SONY, Japan) that generated white noise at full volume. No information was provided regarding the hypotheses in this study, and sufficient rest time was provided between trials to prevent fatigue.

4.2.4 Data Analyses

Synchronization between the user and perturbations was determined through processing of vertical ground reaction forces and valve logic states (ON/OFF). Ground reaction forces of the right leg as collected by the treadmill were processed to determine the instance of heel strike in each cycle. From this information, the timing of each stride and the number of strides per trial was calculated. These were used to

normalize each stride into gait cycle percentages from heel strike of the right leg to the next heel strike of the same leg. The valve logic states were monitored and their timing in the gait cycle (%GC) was calculated.

Each trial was assessed for entrainment success, phase-locking value, variability of phase-locking, consecutive strides in the entrainment window, and strides until the onset of phase-locking. A trial was considered successfully entrained if perturbation timing was confined within a window of ±15 %GC from the running average for at least 50 consecutive strides (phase-locked). This window was referred to as entrainment window. Note that the margin of deviation was expanded to ±15 %GC from the ±10 %GC used in the previous ankle study Thalman *et al.* (2021b) since experimental results sometimes showed a wider variation than ±10 %GC, but still fluctuated about the average, rather than exhibiting the drifting behavior shown in Fig. 3a.

To evaluate how well human gait and the perturbations were synchronized, the mean of absolute deviation from the mean value within the entrainment window was calculated and is referred to as variability of phase-locking. In addition, the number of consecutive strides in the entrainment window was calculated. The number of strides until the onset of phase-locking was quantified to evaluate how quickly a subject can get entrained, which is one important transient characteristic of gait entrainment.

4.2.5 Statistical Analyses

Separate, one-way repeated measures ANOVA tests were preformed to determine statistical dependence on a number of characteristics of interest on perturbation frequency (i.e., frequency level as the within-subject factor) such as phase-locking value, variability of phase-locking, consecutive strides in the entrainment window, and strides until the onset of phase-locking. The assumption of sphericity was for-

mally tested with Mauchly's test of sphericity. When the assumption was violated, the degrees-of-freedom were adjusted using the Greenhouse–Geisser correction before calculating the p-value. Most of these analyses showed statistically insignificant or minimal differences between the six tested perturbation frequencies, and as a result subsequent analyses were performed by aggregating all trials in the same perturbation direction. In addition, paired t-tests were used to identify if those same entrainment characteristics were dependent on perturbation direction.

All statistical tests were made with the SPSS statistical package (IBM, NY) at a significance level of $p < 0.05$. Error bars in result figures and values indicate mean ± 1 standard deviation (SD).

4.3 Results

4.3.1 Success of Entrainment and Phase-Locking

All eleven subjects successfully entrained in every experimental condition: 6 perturbation frequencies ($1.0 \cdot f_{PWS} - 1.15 \cdot f_{PWS}$) in both perturbation directions, thereby confirming the suit could induce gait entrainment to frequencies in excess of a healthy human's natural 'basin of entrainment'. At the start of any given trial, where entrainment had not yet occurred, behavior as in Fig. 3a clearly presented drifting of the perturbation pulse (red lines) across the entire gait phase was observed. After 10+ gait cycles, the perturbation pulse (blue lines) aligned consistently with the toe-off phase for almost all participants (Fig. 3b) demonstrating a strong phase-locking attractor.

The results of a representative subject, which closely reflect the average, are shown in Fig. 4. In each experimental condition, perturbation phase successfully converged to a single final value near toe-off, which aligned with prior studies and confirmed

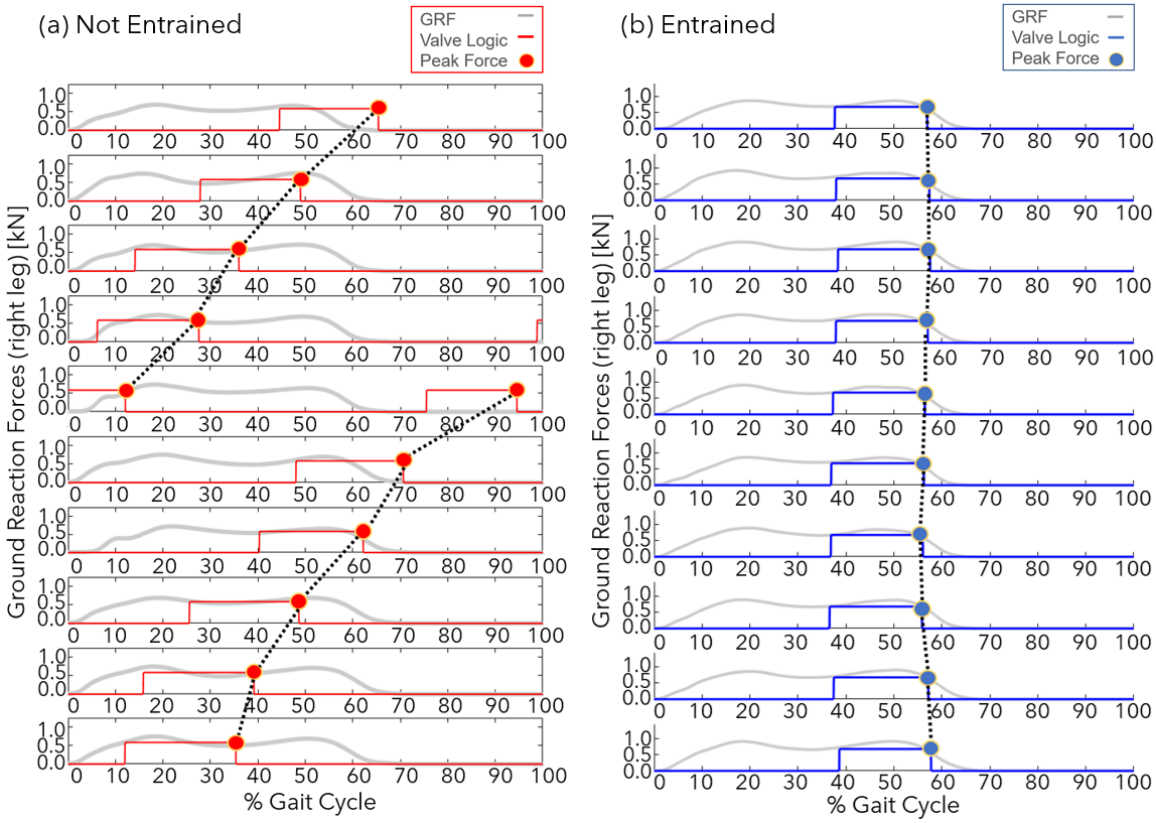

Figure 3: Sample Results of a Representative Subject Showing (a) Not Entrained and (b) Entrained Gait. The Subject's Vertical Ground Reaction Force Was Shown in Grey, and the Actuator Valve Pulse Shown in Red/Blue. (a) Ten Consecutive Gait Cycles in the Initial Transient Phase Where Entrainment Did Not Occur, as Indicated by the Shift in Position of the Perturbation Pulse Peak Across Each of the ten Gait Cycles. (b) Ten Consecutive Entrained Gait Cycles, Where the Perturbation Pulse Consistently Peaks at Around Toe-off.

the existence of a single stable point attractor when unidirectional perturbations are used at the hip.

52.1%±16.7 %GC was the average phase-locking value for extension perturbations, which coincides with the point of peak hip extension in the gait cycle. 63.2%±17.1 %GC was the value for flexion perturbations, which coincides with the transition away from full hip extension towards hip flexion (Fig. 5a). The variability of phase locking, calculated at the average absolute deviation from the phase-locking value, on average was only 3.9±1.2 %GC for flexion trials and was 2.9±0.8 %GC for extension trials, the

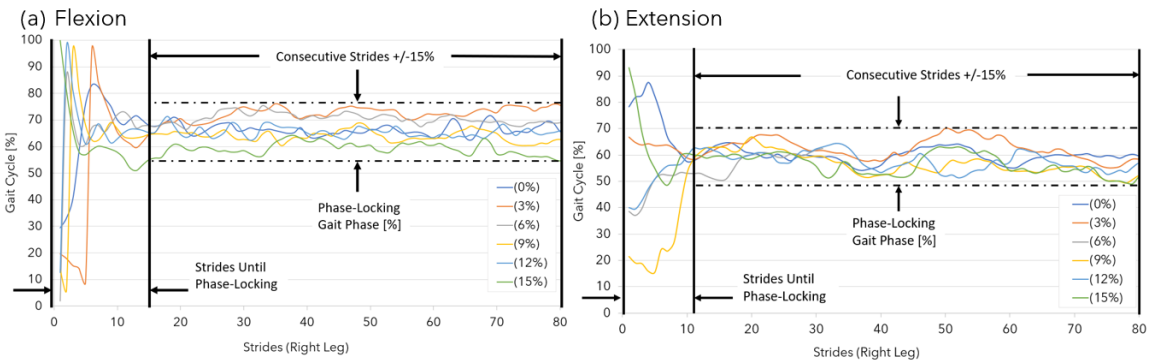

Figure 4: Results of a Representative Subject for (a) Extension Perturbations and (b) Flexion Perturbations for the First 80 Gait Cycles. In All Experimental Conditions, the Initial Transient Response Lasted Only a Few Tens of Gait Cycles. Consistent Phase Locking Around Toe-off Phase Was Observed, Although the Phase-locking Value for Extension Perturbations Was a Bit Earlier than for Flexion Perturbations.

magnitude of which supports the presence of a strong, stable single-point attractor (Fig. 5b). The average number of consecutive entrained strides was 148.2±30.7% and 135.8±34.6% in flexion and extension, respectively (Fig. 5c). The average number of strides taken prior to successful phase-locking 17.2±23.9 and 17.5±17.8 strides for flexion and extension trials respectively (Fig. 5d).

4.3.2 Frequency- and Direction-Dependent Characteristics of Entrainment

Perturbation frequency had statistically insignificant or minimal impact on entrainment characteristics for the same direction of perturbation. Phase-locking value showed no statistical difference across all 6 different frequencies for the flexion perturbation direction ($p = 0.69$) and a marginal difference for the extension perturbation direction ($p = 0.031$). Perturbation frequencies had no significant impact on all other entrainment characteristics: variability of phase-locking for flexion ($p = 0.60$) and extension ($p = 0.93$), consecutive strides in entrainment for flexion ($p = 0.35$) and extension ($p = 0.80$), and strides until the onset of phase-locking for flexion ($p = 0.52$) and extension ($p = 0.75$). Thus, in the follow-up analysis to investigate direction-dependent entrainment characteristics, all trials in the same perturbation direction

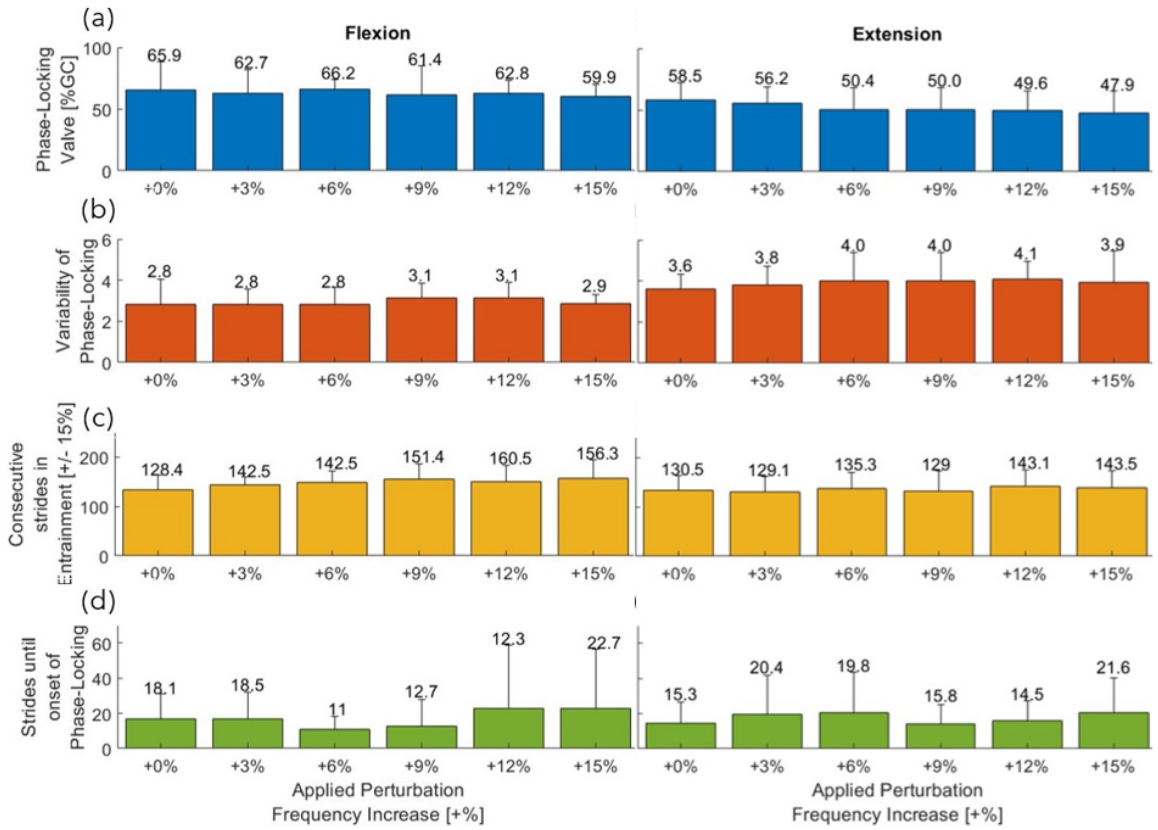

Figure 5: Summary of Average Qualitative Parameters of Interest with the Standard Deviation Across All Participants Shown as Error Bars. From Top to Bottom: The Average Percentage of Gait Cycle at Which Phase-locking Occurred [%GC], the Mean Absolute Deviation from the above Average Phase-locking Value [%GC], the Number of Consecutive Strides Within 15% of the Average Phase-locking Value, and Lastly the Number of Strides until Phase-locking Occurred. Left: Flexion Trials, Right: Extension

were aggregated.

Perturbation direction had significant impact on phase-locking value, variability of phase-locking, and consecutive strides in entrainment, but no impact on strides until the onset of phase-locking. When averaged across all subjects, the phase-locking value for flexion perturbations (63.2 %GC) was significantly later ($p < 0.001$) than that for extension perturbations (52.1 %GC). The variability of phase-locking for flexion perturbations was significantly smaller than for extension perturbations ($p < 0.001$). In addition, the number of consecutive strides in the entrainment window

was significantly longer with flexion perturbations than extension perturbations ($p = 0.003$). However, there was no statistical difference in the strides until the onset of phase-locking between flexion and extension data ($p = 0.95$).

4.4 Discussion

The motivation of this study was to investigate the potential of a soft robotic hip exosuit (SR-HExo) to expand the current capabilities of gait entrainment. The study recruited 11 subjects to walk with the SR-HExo for a series of 12 trials with varying perturbation directions and frequencies, and monitored the average phase-locking value, variability of phase-locking, consecutive strides within the entrainment window, and the number of strides until the onset of phase-locking. All 11 subjects exhibited successful entrainment to perturbations significantly faster than 15% of their preferred gait frequency after an average of 17.5 strides. These results, coupled with its low-weight and modular structure, support the use of the SR-HExo as an effective tool to induce gait entrainment.

In all experimental conditions, all subjects consistently showed a single phase-locking value around the toe-off phase, confirming the existence of a single stable point when unidirectional perturbations were applied to the hip joint. This result is consistent with previous ankle studies Ahn and Hogan (2012); Ochoa *et al.* (2017); Thalman *et al.* (2021b). Phase-locking at two distinct gait phases (one around toe-off and the other during mid-swing) in the previous hip entrainment study is likely due to the use of flexion perturbation on one leg and extension perturbation on the other leg in a single session Lee *et al.* (2019).

The previous gait entrainment study with hip perturbations utilized a rigid hip exoskeleton robot that weighed 2.1 kg. It applied trapezoidal torque perturbations with a peak torque of 6 Nm in flexion (right leg) and extension (left leg), acting in

opposite directions, at a rate around 2-3% greater than the preferred gait frequency while walking overground for 80 consecutive strides Lee *et al.* (2019). Only 72.5% of the trials in this study featured successful entrainment in comparison to 100% success with the SR-HExo in the current study even with substantially higher perturbation frequencies (i.e., up to 15% greater than the preferred gait frequency), which demonstrates the potential use of the SR-HExo to extend the basin of entrainment. The current study also showed faster transient entrainment behavior compared to the previous study. While the number of strides until the onset of phase locking in the current study was 17.3±20.6 strides on average, the previous study with the rigid hip exoskeleton robot frequently required over 50 strides until phase-locking was achieved. Improved performance with the SR-HExo in terms of success rate of entrainment, basin of entrainment, and transient entrainment behavior together supports its potential use to enhance gait entrainment characteristics.

Phase-locking occurred significantly sooner in the gait cycle with extension perturbations than with flexion perturbations. On average, extension perturbations occurred at 52.1 %GC, near full hip extension, and flexion perturbations occurred at 63.2 %GC, at the transition from full hip extension towards hip flexion. These perturbations aligned with the gait phase where they could provide mechanical assistance for hip movement. Hip extension perturbations on average occurred at the end of stance phase, where they assisted with push-off, and hip flexion perturbations occurred just after toe-off where they assisted the hip in transitioning from peak extension to flexion. The results of having a potential benefit of assistance from mechanical perturbations are consistent with previous ankle studies Ahn and Hogan (2012); Ochoa *et al.* (2017); Thalman *et al.* (2021b).

It is worth to note that phase-locking did not occur in other gait phases than around toe-off, even where perturbations could better assist hip movement. For ex-

ample, maximum hip flexion torque occurs in the late swing and early stance phases Grimmer *et al.* (2014), but phase-locking did not occur in these phases. This indicates mechanical assistance might not be the only factor determining phase-locking timing in gait entrainment. In fact, previous gait entrainment studies using electrical perturbations on gastrocnemius demonstrated that entrainment can occur even with electrical stimulation that is too weak to induce significant assistive torque or mechanical benefit Nishimura *et al.* (2018); Thorp and Adamczyk (2020). One potential explanation for this may be that sensory cues are also an important factor for gait entrainment. Another potential explanation is that the human neuromuscular system might simply find the best time to easily reject external disturbances (perturbations) in order to maintain natural gait biomechanics, and the phase around toe-off might be the case.

Comparison of results for two different perturbation directions suggests that flexion perturbations may be better suited for their implementation in rehabilitation settings than those applied in extension. The variability of phase-locking, quantified by the mean absolute deviation from the phase-locking value, on average was smaller with flexion perturbations (2.9±0.8 %GC) than with extension perturbations (3.9±1.2 %GC). In addition, flexion perturbations induce entrainment for more consecutive strides on average (148.2±30.7) than extension perturbations (135.8±34.6). The differences of these two metrics were statistically significant.

Chapter 5

CONCLUSIONS & FUTURE SCOPE

5.0.1 Conclusions

A robotic exosuit made from compliant materials and actuators was tested for its ability to reduce hip flexor and extensor muscle activity for locomotor assistance and induce entrainment in healthy individuals beyond the 7% natural basin of entrainment. The payload capacity of the suit actuators were characterized in both static and dynamic tests in parallel (dual ff-PAM) and crossed (X-ff-PAM) orientations. These orientations preformed comparably in test as the parallel orientation delivered a 189.2±8.2 N payload when inflated to 200 kPa over 0.3 seconds, and X-ff-PAM delivered a 191.2±4.6 N payload - both within ±10% of the 200N force requirement for hip flexion assistance. The X-ff-PAM actuators were utilized in the development of this suit to maximize range of motion retention at the hip and maximize suit force output.

In the assistance-assessment experiment, three healthy adults walked on a treadmill monitored with motion capture and sEMG under three experimental conditions: no exosuit, passive exosuit, and active exosuit. In the active exosuit condition, the anterior actuators were engaged between toe-off to terminal swing to reduce muscular effort in hip flexion, and the posterior actuators were engaged between stance-phase and toe-off to reduce muscular effort in hip extension. Hip ROM was only reduced by 4^o out of a target of 30^o, implying this suit would not hinder the full range of movement for impaired individuals, who often have a range of motion much smaller than that of healthy adults (for hip replacement patients, hip ROM may be less than

25^o) Perron *et al.* (2000). Significant reductions were seen in sEMG data for both hip flexors (the iliacus and rectus femoris) and both hip extensors (gluteus maximus and biceps femoris), which are promising results for the suits potential to provide statistically significant locomotor assistance without impacting natural gait kinematics.

In the entrainment induction experiment, 11 healthy adults walked on a treadmill wearing a modified SR-HExo suit for a series of 12 trials with varying perturbation directions and frequencies, with the average phase-locking value, variability of phase-locking, consecutive strides within the entrainment window, and the number of strides until the onset of phase-locking monitored via force plate and valve signal data. All participants successfully experienced entertainment in all test conditions, including and up to perturbations 15% faster than their preferred walking speed, after an average of 17.5 strides. All participants consistently entrained to a small range of %GC values around toe-off in all test conditions, indicating toe-off is the single stable attractor for entrainment behavior induced at the hip with unidirectional perturbations. These results are consistent with ankle perturbation studies Ahn and Hogan (2012); Ochoa *et al.* (2017); Thalman *et al.* (2021b). In extension data averaged across all subjects, perturbations occurred at 52.1 %GC, near full hip extension. In flexion data averaged across all subjects, flexion perturbations occurred at 63.2 %GC, just after full hip extension to assist the transition to flexion. The potential mechanical assistance provided by perturbations at these times are consistent with previous ankle studies as well Ahn and Hogan (2012); Ochoa *et al.* (2017); Thalman *et al.* (2021b). However, it should be noted that perturbations could theoretically better assist hip movement in flexion during the point of maximum flexion torque in the late swing and early stance phases Grimmer *et al.* (2014) as the suit was used in the assistance study Thalman *et al.* (2021a), but phase-locking did not occur in these phases. This suggests that mechanical assistance may not be the only determining

factor in phase-locking timing in gait entrainment which is consistent with a previous ankle study that utilized weak electrical perturbations applied to the gastrocnemius that provided no mechanical benefit Nishimura *et al.* (2018); Thorp and Adamczyk (2020). Theories for the fundamental truth of phase-locking timing include alignment to other sensory cues, or perhaps that human neuromuscular systems reject external disturbances to toe-off, where natural gait biomechanics are the least impacted.

5.0.2 Next Steps

The SR-HExo worn component is the lightest low-profile lower body exosuit/ exoskeleton with both assistive and rehabilitative potential in the state of the art, a landmark among a large field of medical devices for use in clinical contexts Asbeck *et al.* (2015); Ding *et al.* (2014, 2016); Lee *et al.* (2019); Lewis and Ferris (2011); Martini *et al.* (2019); Quintero *et al.* (2011); Tefertiller *et al.* (2018); Thakur *et al.* (2018b); Wehner *et al.* (2013); Young and Ferris (2017). The SR-HExo is fabricated from heat-sealed fabric, neoprene, and nylon fabrics which contain minimal moving and electrified parts, preventing the pinching and shearing injuries possible with cable and motor-driven systems. Both studies of this device were limited to healthy participants, and the device fits most users without major adjustments. The suit does not fit users with legs shorter than 0.71 m and small modifications must be made to the hip anchor, leg anchor, and actuator attachments. For use in assistance, further investigation is required to monitor transient exosuit integrity and transient impact of exosuit use (if any) on hip biomechanics. For use in rehabilitation, further work will determine the maximum extent to which this suit can expand the basin of entrainment of healthy subjects as in Thalman *et al.* (2021b), by applying progressively faster perturbations until entrainment failure. In addition, the impact of treadmill versus overground walking must be explored as well as a modelling study

of the neuromuscular mechanisms of gait entrainment to hip-located perturbations.

REFERENCES

Ahn, J. and N. Hogan, "Feasibility of dynamic entrainment with ankle mechanical perturbation to treat locomotor deficit", in "2010 Annual International Conference of the IEEE Engineering in Medicine and Biology", pp. 3422–3425 (IEEE, 2010).

Ahn, J. and N. Hogan, "Walking is not like reaching: evidence from periodic mechanical perturbations", PloS one **7**, 3, e31767 (2012).

Ahn, J., T. Patterson, H. Lee, D. Klenk, A. Lo, H. I. Krebs and N. Hogan, "Feasibility of entrainment with ankle mechanical perturbation to treat locomotor deficit of neurologically impaired patients", in "2011 Annual international conference of the IEEE engineering in medicine and biology society", pp. 7474–7477 (IEEE, 2011).

Alonso, A., F. H. J. Aparicio, E. J. Benjamin, M. S. Bittencourt, C. W. Callaway, F. A. P. Carson, F. A. M. Chamberlain, B. M. Kissela, F. K. L. Knutson, C. D. Lee *et al.*, "Heart disease and stroke statistics—2021 update", Circulation **2021**, 143, e00–e00 (2021).

Androwis, G. J., R. Pilkar, A. Ramanujam and K. J. Nolan, "Electromyography assessment during gait in a robotic exoskeleton for acute stroke", Frontiers in neurology **9**, 630 (2018).

Asbeck, A. T., S. M. De Rossi, K. G. Holt and C. J. Walsh, "A biologically inspired soft exosuit for walking assistance", International Journal of Robotics Research (2015).

Baylor, C., K. M. Yorkston, M. P. Jensen, A. R. Truitt and I. R. Molton, "Scoping review of common secondary conditions after stroke and their associations with age and time post stroke", Topics in stroke rehabilitation **21**, 5, 371–382 (2014).

Bennett, M., M. Schatz, H. Rockwood and K. Wiesenfeld, "Huygens ' s clocks", Proc. R. Soc. Lond. A **458**, 563–579 (2002).

Bonnefoy-Mazure, A. and S. Armand, *Orthopedic management of children with cerebral palsy*, vol. 40, chap. 16: Normal, p. 645–657 (Nova Science Publishers, Inc., 2015).

Booth, F. W., C. K. Roberts and M. J. Laye, "Lack of exercise is a major cause of chronic diseases", Comprehensive physiology **2**, 2, 1143 (2012).

Brandstater, M. E., H. de Bruin, C. Gowland and B. M. Clark, "Hemiplegic gait: analysis of temporal variables.", Archives of physical medicine and rehabilitation **64**, 12, 583–587 (1983).

Buesing, C., G. Fisch, M. O'Donnell, I. Shahidi, L. Thomas, C. K. Mummidisetty, K. J. Williams, H. Takahashi, W. Z. Rymer and A. Jayaraman, "Effects of a wearable exoskeleton stride management assist system (sma®) on spatiotemporal gait characteristics in individuals after stroke: a randomized controlled trial", Journal of neuroengineering and rehabilitation **12**, 1, 1–14 (2015).

Cao, J., S. Q. Xie, R. Das and G. L. Zhu, "Control strategies for effective robot assisted gait rehabilitation: the state of art and future prospects", Medical engineering & physics **36**, 12, 1555–1566 (2014).

Ding, Y., I. Galiana, A. Asbeck, B. Quinlivan, S. M. M. De Rossi and C. Walsh, "Multi-joint actuation platform for lower extremity soft exosuits", in "2014 IEEE International Conference on Robotics and Automation (ICRA)", pp. 1327–1334 (Ieee, 2014).

Ding, Y., I. Galiana, A. T. Asbeck, S. M. M. De Rossi, J. Bae, T. R. T. Santos, V. L. De Araujo, S. Lee, K. G. Holt and C. Walsh, "Biomechanical and physiological evaluation of multi-joint assistance with soft exosuits", IEEE Transactions on Neural Systems and Rehabilitation Engineering **25**, 2, 119–130 (2016).

Farris, D. J. and G. S. Sawicki, "The mechanics and energetics of human walking and running: a joint level perspective", Journal of The Royal Society Interface **9**, 66, 110–118 (2012).

Grimmer, M., M. Eslamy and A. Seyfarth, "Energetic and peak power advantages of series elastic actuators in an actuated prosthetic leg for walking and running", in "Actuators", vol. 3, pp. 1–19 (Multidisciplinary Digital Publishing Institute, 2014).

Hsu, A.-L., P.-F. Tang and M.-H. Jan, "Analysis of impairments influencing gait velocity and asymmetry of hemiplegic patients after mild to moderate stroke", Archives of physical medicine and rehabilitation **84**, 8, 1185–1193 (2003).

Kim, C. M. and J. J. Eng, "Symmetry in vertical ground reaction force is accompanied by symmetry in temporal but not distance variables of gait in persons with stroke", Gait & posture **18**, 1, 23–28 (2003).

Knight, J. A., "Physical inactivity: associated diseases and disorders", Annals of Clinical & Laboratory Science **42**, 3, 320–337 (2012).

Knutsson, E. and C. Richards, "Different types of disturbed motor control in gait of hemiparetic patients.", Brain: a journal of neurology **102**, 2, 405–430 (1979).

Lee, J., D. Goetz, M. E. Huber and N. Hogan, "Feasibility of gait entrainment to hip mechanical perturbation for locomotor rehabilitation", in "2019 IEEE/RSJ International Conference on Intelligent Robots and Systems (IROS)", pp. 7343–7348 (IEEE, 2019).

Lewis, C. L. and D. P. Ferris, "Invariant hip moment pattern while walking with a robotic hip exoskeleton", Journal of Biomechanics **44**, 5, URL `http://dx.doi.org/10.1016/j.jbiomech.2011.01.030` (2011).

Martini, E., S. Crea, A. Parri, L. Bastiani, U. Faraguna, Z. McKinney, R. Molino-Lova, L. Pratali and N. Vitiello, "Gait training using a robotic hip exoskeleton improves metabolic gait efficiency in the elderly", Scientific reports **9**, 1, 1–12 (2019).

Merletti, R. and P. Di Torino, "Standards for reporting emg data", J Electromyogr Kinesiol **9**, 1, 3–4 (1999).

Mizelle, C., M. Rodgers and L. Forrester, "Bilateral foot center of pressure measures predict hemiparetic gait velocity", Gait & posture **24**, 3, 356–363 (2006).

Nishimura, K., E. Martinez, A. Loeza, J. Parker and S.-J. Kim, "Effects of periodic sensory perturbations during electrical stimulation on gait cycle period", PloS one **13**, 12, e0209781 (2018).

Ochoa, J., D. Sternad and N. Hogan, "Treadmill vs. overground walking: different response to physical interaction", Journal of neurophysiology **118**, 4, 2089–2102 (2017).

Olney, S. J., M. P. Griffin and I. D. McBride, "Temporal, kinematic, and kinetic variables related to gait speed in subjects with hemiplegia: a regression approach", Physical therapy **74**, 9, 872–885 (1994).

Patterson, K. K., I. Parafianowicz, C. J. Danells, V. Closson, M. C. Verrier, W. R. Staines, S. E. Black and W. E. McIlroy, "Gait asymmetry in community-ambulating stroke survivors", Archives of physical medicine and rehabilitation **89**, 2, 304–310 (2008).

Perron, M., F. Malouin, H. Moffet and B. J. McFadyen, "Three-dimensional gait analysis in women with a total hip arthroplasty", Clinical Biomechanics **15**, 7, 504–515 (2000).

Power, V., L. O'Sullivan, A. de Eyto, S. Schülein, C. Nikamp, C. Bauer, J. Mueller and J. Ortiz, "Exploring user requirements for a lower body soft exoskeleton to assist mobility", in "Proceedings of the 9th ACM International Conference on PErvasive Technologies Related to Assistive Environments", pp. 1–6 (2016).

Quintero, H., R. Farris, C. Hartigan, I. Clesson and M. Goldfarb, "A powered lower limb orthosis for providing legged mobility in paraplegic individuals", Topics in spinal cord injury rehabilitation **17**, 1, 25–33 (2011).

Quintero, H. A., R. J. Farris, C. Hartigan, I. Clesson and M. Goldfarb, "A Powered Lower Limb Orthosis for Providing Legged Mobility in Paraplegic Individuals", Top Spinal Cord Injury Rehabiliation **17**, 1, 25–33 (2012).

Riener, R., L. Lunenburger, S. Jezernik, M. Anderschitz, G. Colombo and V. Dietz, "Patient-cooperative strategies for robot-aided treadmill training: first experimental results", IEEE transactions on neural systems and rehabilitation engineering **13**, 3, 380–394 (2005).

Rodríguez-Fernández, A., J. Lobo-Prat and J. M. Font-Llagunes, "Systematic review on wearable lower-limb exoskeletons for gait training in neuromuscular impairments", Journal of neuroengineering and rehabilitation **18**, 1, 1–21 (2021).

Sezer, N., S. Akkuş and F. G. Uğurlu, "Chronic complications of spinal cord injury", World journal of orthopedics **6**, 1, 24 (2015).

Tefertiller, C., K. Hays, J. Jones, A. Jayaraman, C. Hartigan, T. Bushnik and G. F. Forrest, "Initial outcomes from a multicenter study utilizing the indego powered exoskeleton in spinal cord injury", Topics in spinal cord injury rehabilitation **24**, 1, 78–85 (2018).

Thakur, C., K. Ogawa, T. Tsuji and Y. Kurita, "Soft wearable augmented walking suit with pneumatic gel muscles and stance phase detection system to assist gait", IEEE Robotics and Automation Letters **3**, 4, 4257–4264 (2018a).

Thakur, C., K. Ogawa, T. Tsuji and Y. Kurita, "Soft Wearable Augmented Walking Suit With Pneumatic Gel Muscles and Stance Phase Detection System to Assist Gait", IEEE Robotics and Automation Letters 2018 IEEE/RSJ International Conference on Intelligent Robots and Systems (IROS) **3**, 4, 4257–4264 (2018b).

Thalman, C. and P. Artemiadis, "A review of soft wearable robots that provide active assistance: trends, common actuation methods, fabrication, and applications", Wearable Technologies **1** (2020).

Thalman, C. M., L. Baye-Wallace and H. Lee, "A Soft Robotic Hip Exosuit (SR-HExo) to Assist Hip Flexion and Extension during Human Locomotion", in "2021 IEEE/RSJ International Conference on Intelligent Robots and Systems (IROS)", (2021a).

Thalman, C. M., M. Debeurre and H. Lee, "Entrainment during human locomotion using a soft wearable ankle robot", IEEE Robotics and Automation Letters **6**, 3, 4265–4272 (2021b).

Thalman, C. M., T. Hertzell and H. Lee, "Toward a soft robotic ankle-foot orthosis (sr-afo) exosuit for human locomotion: Preliminary results in late stance plantarflexion assistance", in "2020 3rd IEEE International Conference on Soft Robotics (RoboSoft)", pp. 801–807 (IEEE, 2020).

Thalman, C. M., J. Hsu, L. Snyder and P. Polygerinos, "Design of a soft ankle-foot orthosis exosuit for foot drop assistance", in "2019 International Conference on Robotics and Automation (ICRA)", pp. 8436–8442 (IEEE, 2019).

Thorp, J. E. and P. G. Adamczyk, "Mechanisms of gait phase entrainment in healthy subjects during rhythmic electrical stimulation of the medial gastrocnemius", Plos one **15**, 10, e0241339 (2020).

Webster, J. B. and B. J. Darter, "Principles of normal and pathologic gait", in "Atlas of Orthoses and Assistive Devices", pp. 49–62 (Elsevier, 2019).

Wehner, M., B. Quinlivan, P. M. Aubin, E. Martinez-Villalpando, M. Baumann, L. Stirling, K. Holt, R. Wood and C. Walsh, "A lightweight soft exosuit for gait assistance", in "2013 IEEE international conference on robotics and automation", pp. 3362–3369 (IEEE, 2013).

Wesseling, M., F. De Groote, C. Meyer, K. Corten, J.-P. Simon, K. Desloovere and I. Jonkers, "Gait alterations to effectively reduce hip contact forces", Journal of Orthopaedic Research **33**, 7, 1094–1102 (2015).

Winter, D. A., "Overall principle of lower limb support during stance phase of gait", Journal of biomechanics **13**, 11, 923–927 (1980).

Yang, A., P. Asselin, S. Knezevic, S. Kornfeld and A. M. Spungen, "Assessment of in-hospital walking velocity and level of assistance in a powered exoskeleton in persons with spinal cord injury", Topics in Spinal Cord Injury Rehabilitation **21**, 2, 100–109 (2015).

Young, A. J. and D. P. Ferris, "State of the art and future directions for lower limb robotic exoskeletons", IEEE Transactions on Neural Systems and Rehabilitation Engineering **25**, 2, 171–182 (2017).

This work was submitted for publication in IEEE Robotics and Automation Letters (RA-L 2022) and was also accepted for presentation at IEEE/RSJ's International Conference on Intelligent Robotics and Systems (IROS 2021) in Sepetember 2021, Prague, Czech Republic. This published work was co-authored by Dr. Hyunglae Lee and Dr. Carly Thalman who have granted permission to Lily Baye-Wallace to publish this work as her thesis.

In reference to IEEE copyrighted material, which is used with permission in this thesis, the IEEE does not endorse any of Arizona State University's products or services. Internal or personal use of this material is permitted